Effects of beam axial deformations on storey-based critical gravity loads in tension-only semi-braced steel frames

Terence Ma[1], Linbo Zhang[1], Lei Xu[1]

[1]Department of Civil and Environmental Engineering, University of Waterloo, 200 University Avenue West, Waterloo, ON., N2L 3G1, Canada

Corresponding Author:
Lei Xu, University of Waterloo
200 University Avenue West
Waterloo, ON. N2L 3G1
Tel: (519) 888-4567 x36882
Email: lxu@uwaterloo.ca

Abstract

If the beams in a structural frame are not connected to slabs or other rigid diaphragms, the beams will axially deform when the frame is subjected to lateral loads, reducing the critical loads and increasing local deflections in the structure. The consideration of beam axial deformations always reduces the lateral stiffness of the frame, but has so far been neglected in storey-based stability methods. The lateral stiffness of a semi-braced (tension-only), semi-rigidly connected steel frame accounting for the axial deformations in its connecting beams is derived in this paper. The equations also apply to unbraced frames and/or idealized connections, which are commonly encountered or assumed in practice. It is demonstrated that the effect of beam axial deformation on the lateral stiffness of the frame can conveniently be accounted for using the concept of equivalent series and parallel springs. A lateral stiffness reduction factor is also introduced to predict the effects of beam axial deformations. The theoretical accuracy of the proposed method is verified via finite element analysis and the method is demonstrated via numerical examples. The effect of beam axial deformations on the critical gravity loads of frames was found to be significant in some cases, especially when the ratio of beam axial stiffness to column lateral stiffness is small – that is, within the order of 10^2. However, axial beam deformations have negligible effects on the critical gravity loads if the ratio is sufficiently large or where rotational buckling governs the failure mode, within the order of 10^3 or above.

Keywords: axial deformations; semi-braced; steel frame; lateral stability; semi-rigid; buckling

1 Introduction

The prevention of instability in the design of structural frames is of primary importance. The topic of storey-based stability in steel frames has been continually investigated over the last few decades [1-16]. Although neglected in the proposed methods found in the literature, the effects of axial deformations in beams have the potential to significantly reduce the critical gravity loads of steel frames. Particularly, axial deformations occur in beams if the beams are not connected to slabs or other rigid diaphragms, causing a reduction to the storey-based lateral stiffness compared to when the beams are assumed to be axially rigid. In other words, with the assumption of rigid floor diaphragms in which all columns in the same storey have an identical lateral deformation, the possible axial deformation of beams is neglected. Whereas this assumption may be accepted for residential, institutional and commercial building frameworks because of the presence of concrete slabs, it may not be valid for frameworks such as single-storey industrial or warehouse buildings in which the roof diaphragms are relatively flexible. For this reason, the axial deformation of beams needs to be considered in the stability analysis.

In this study, a method is derived for calculating the lateral stiffness of a storey frame accounting for axial deformations in beams. It was found that the evaluation of stability via quantification of the lateral stiffness of a storey frame can be conveniently achieved using the concept of equivalent parallel and series spring stiffness [17-18]. The proposed method is a generalization of the Xu & Liu [6] method for computing the lateral stiffness of a semi-braced or unbraced, semi-rigidly or ideally connected frame, which does not originally account for the axial deformations in beams. Semi-braced frames are defined as those with limited amounts of lateral bracing present but still experience significant lateral sway in the buckling mode. Semi-braced frames will have higher axial loading capacities and reduced lateral deflections when compared to equivalent unbraced frames with the lateral bracing removed. The semi-braced case for a frame reflects a transition between the fully-unbraced and fully-braced cases [19-20]. Note that this study considers only tension-only bracing, which is common in applications of steel frames for single-storey industrial, commercial and warehouse buildings. The proposed method also considers

semi-rigid connections between the members, as connections are never completely pinned or rigid in reality. Of course, the proposed method also applies to idealized connections.

A new reduction factor to the lateral stiffness to predict the effects of axial deformations in beams is also introduced. To be consistent with the method developed by Xu & Liu [6], the proposed method also accounts for the reduction in lateral stiffness of columns due to axial loads via P-Δ effects. The theoretical accuracy of the derived method is verified via finite element analysis. In fact, the proposed equations represent a closed solution to the system of differential equations representing the deformable behaviour of the system. The solution is simple to understand, and relates the stiffness of the structure directly to the variables in the equations, allowing for comprehensive understanding of the problem. While numerical solutions such as finite element analyses may be difficult to understand for many practitioners and can potentially lead to the improper assignment of input variables. An advantage of the proposed method is to provide a methodology for performing the same stability analyses under a relatively simplistic theoretical basis, as it employs the more commonly understood concept of springs in parallel and series. Numerical examples are presented to demonstrate the use of the approach and the results are compared with the results obtained from Xu & Liu [6] in order to assess the effect of beam axial deformations on the critical gravity loads of the frames.

2 Background

Yura [1] initiated the notion of storey-based stability by identifying that the instability of a single storey requires all columns within the storey to buckle simultaneously. LeMessurier [2] and Lui [3] subsequently used the concept to develop matrix-based methods for evaluating storey-based stability. Following this, Aristizabal-Ochoa [4] and Xu [5-6] developed closed-form equations for evaluating storey-based stability. Other researchers [7-10] have since developed various similar methods for estimating the storey-based critical loads of storey frames. The effect of interactions between adjoining members across multiple storeys towards the computation of storey-based stability has also recently been investigated [11-14]. Finally, the storey-based stability method has been extended to account for temperature effects [15] and

shear deformations [16]. However, unlike the current study none of the above studies have considered the effect of axial deformations towards the critical loads of the frames.

The focus of this study begins by drawing attention to the Xu & Liu [6] method, which was the first to extend the Yura [1] method towards considering the *P*-Δ effect in reducing the lateral stiffness of planar storey frames containing semi-rigid connections, shown in Fig. (1).

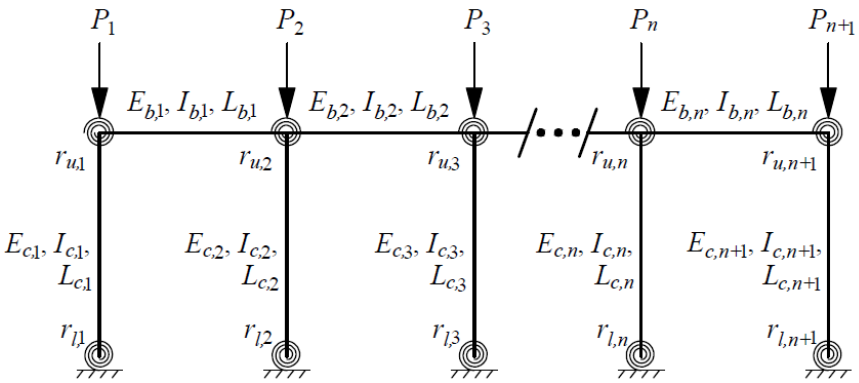

Figure 1 – General storey frame subjected to gravity loading

The planar frame is subjected to applied gravity loads, P_i. Out-of-plane effects are not considered in storey-based stability methods. Let the indices *i* and *j* correspond to the numbering of the columns and beams, respectively, from left to right. Similarly, the subscripts *c* and *b* are designated to columns and beams, respectively, and *n* is the number of bays. The elastic modulus, moment of inertia and length of each member are *E*, *I*, and *L*, respectively. For the purpose of generalization, all connections can be modelled as rotational springs, and the effective column lower- and upper-end fixity factors are r_l and r_u, respectively. The end fixity factors are measures of the rotational rigidity at corresponding ends of the member, originally defined in [21] and shown in Eqs. (1). The research on the rotational stiffness behaviour of semi-rigid connections has since grown in popularity [22] over the past few decades [5-6, 8, 12, 22-27].

$$r_{u,i} = \frac{1}{1+3E_{c,i}I_{c,i}/R_{u,i}L_{c,i}}; \quad R_{u,i} = \sum_{j_u=1}^{m_u} R_{i,j_u} \tag{1a}$$

$$r_{l,i} = \frac{1}{1+3E_{c,i}I_{c,i}/R_{l,i}L_{c,i}}; \quad R_{l,i} = \sum_{j_l=1}^{m_l} R_{i,j_l} \tag{1b}$$

where R_u and R_l are the rotational stiffness of the upper- and lower-end connections of the column, respectively. With using this model it is assumed that the end rotational restraints are not affected by axial loads. The end fixity factors can also be applied for idealized connections. The end fixity factors are defined such at $r = 0$ represents a pinned-end connection and $r = 1$ represents a fixed-end connection. Intermediate values of r between zero and unity can be used to characterize semi-rigid connections. The rotational restraint provided by beam j to column i at the corresponding end, $R_{i,j}$, can be calculated using Eq. (2) as follows [5].

$$R_{i,j} = \frac{6E_{b,j}I_{b,j}r_{N,j}}{L_{b,j}}\left[\frac{2+v_{FN}r_{F,j}}{4-r_{N,j}r_{F,j}}\right] \tag{2}$$

where $r_{N,j}$ and $r_{F,j}$ are the end-fixity factors for the near and far ends of beam j connected to column i, and v_{FN} is the ratio of rotation of the far end connection of the beam, θ_F, to the rotation of the near end connection of the beam, θ_N. Xu & Liu [6] demonstrated that accurate estimations of results can be obtained by assuming the case of asymmetric buckling, $v_{FN} = 1$, for partially restrained and unbraced frames. Xu & Liu [6] showed that the lateral stiffness of the frame in Fig. (1), considering only the flexural deformations of members while ignoring the effects of shear and axial deformations in the members, can be calculated using Eq. (3). For convenience, a theoretical basis for this equation is also provided in Appendix A.

$$\Sigma S = \Sigma K_{br} + \sum_{i=1}^{n+1} S_{c,i} = \Sigma K_{br} + \sum_{i=1}^{n+1} \frac{12E_{c,i}I_{c,i}}{L_{c,i}^3}\beta_i(\phi_i, r_{l,i}, r_{u,i}) \tag{3}$$

Where ΣS is the lateral stiffness of the storey frame, taken as the sum of the lateral stiffness of each column, $S_{c,i}$, and ΣK_{br} is the lateral bracing stiffness of the frame provided by tension-only braces. The β_i factor accounts for second-order effects, shown in Eqs. (4).

$$\beta = \frac{\phi^3}{12}\frac{a_1\phi\cos\phi + a_2\sin\phi}{18r_l r_u - a_3\cos\phi + (a_1 - a_2)\phi\sin\phi} \tag{4a}$$

$$a_1 = 3[r_l(1-r_u) + r_u(1-r_l)] \tag{4b}$$

$$a_2 = 9r_l r_u - (1-r_l)(1-r_u)\phi^2 \tag{4c}$$

$$a_3 = 18r_l r_u + a_1\phi^2 \tag{4d}$$

Where $\phi_i = L_i\sqrt{P_i / E_i I_i}$ is the axial load coefficient. β_i is a monotonically decreasing function of the axial compressive load, and indicates whether the column is sufficiently stable on its own ($\beta > 0$) or relies on the lateral stiffness of other columns in the storey to maintain stability ($\beta \leq 0$). In assuming that all of the columns have the same lateral deformation (effectively acting as springs in parallel), the frame will be laterally stable if $\Sigma S > 0$, and unstable when ΣS diminishes to zero since theoretically the lateral deformations would approach infinity.

The above formulation adopts the assumption that all of the columns deflect by the identical lateral displacement. However, this assumption implies that the beams are connected to rigid diaphragms and effectively possess infinite axial stiffness, which can be non-conservative for cases where the rigid diaphragms are not available. The storey-based stability approach was developed based on the consideration of rigid-floor or roof diaphragms, which mimics the reality of practical building construction. When applying the storey-based stability approach to the cases with non-rigid (flexible) diaphragms or no diaphragm present, the approach may not be conservative due to neglecting the axial deformation of the beam. In fact, the research on storey-based stability performed on semi-braced frames thus far [1,4-6,11,15-16] have assumed the presence of rigid diaphragms. Similarly, existing storey-based stability analysis methods for unbraced and braced frames [1,9,14,27,32] have also assumed the presence of rigid diaphragms. As such, the aforementioned methods may yield non-conservative results for the critical gravity loads of the frames. To address this shortcoming, the storey-based lateral stiffness equation for semi-braced (and unbraced), semi-rigidly (or ideally) connected steel frames with flexible or no diaphragms is derived in this study.

Using the proposed method, the lateral stiffness of a storey can be determined by applying the concept of equivalent springs. As discussed in [17-18], the concept of equivalent springs is rarely used in static analyses of structural systems but is useful for relating fundamental mechanics concepts to the analysis of complex structural systems. Although dynamic structural systems are often modelled in terms of equivalent springs [28-30], the same concept remains surprisingly uncommon in the field of static

structural analysis of buildings despite the capability of the concept to be applied towards the evaluation of structural stability as demonstrated in this paper. The concept is technically utilized in some current storey-based stability methods [5-6, 13, 15-16], but which only deal with the aforementioned assumption that all columns in a storey laterally deflect with the same lateral deformation. Effectively, the columns are thus treated as springs in parallel but the beams, which can axially deform, are not considered in any of these storey-based stability models [5-6, 13, 15-16].

It is noted that multi-storey frames can be analysed using storey-based methods via decomposition into individual storeys, which are analyzed separately. The extension of the storey-based stability approach in [6] has been accomplished in this manner by [11]. However, the application of the proposed method to consider the effects of beam axial deformations in multi-storey frames directly without modifications may result in small errors in the critical loads, because the bases of the columns in the storey are assumed to be restricted from differential translations in the lateral direction. For multi-storey frames, this assumption may not be true if the floor below is not rigid, and continual research is being conducted to verify the applicability of the proposed approach towards multi-storey frames [33]. In any case, multi-storey frames often contain rigid diaphragms which can be analyzed using previous storey-based stability methods. Regardless, the proposed method is a significant milestone towards the goal of considering beam axial effects in multi-storey frames.

3 Storey-Based Stability Considering the Effects of Beam Axial Deformations

The lateral stiffness of a semi-braced frame containing semi-rigid connections and considering the effect of beam axial deformations is derived in this section. A lateral load, Q, is applied on the upper end of the left-most column of the n-bay frame shown in Fig. (2). In addition, each column in the frame is subjected to an applied load, P_i.

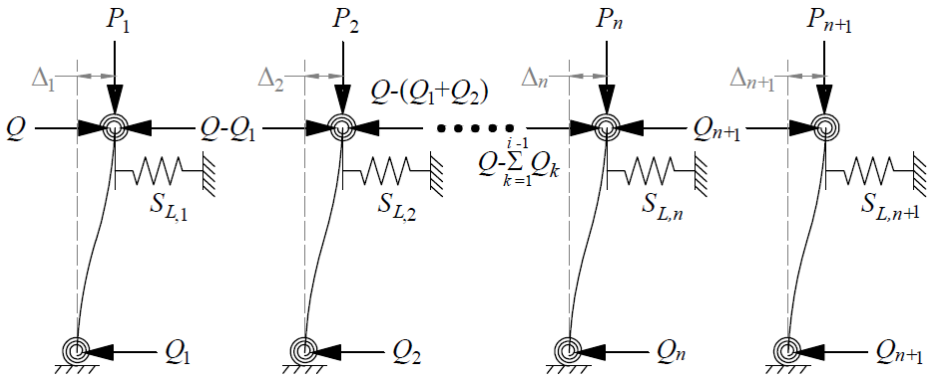

Figure 2 – Semi-braced storey frame subjected to gravity loading

The lateral load Q is distributed to each column via the reactions Q_i in Eq. (5). Note that even if Q is not present, based on the buckling shape of the frame there will still be axial forces in the beams related to the reactions Q_i. Also, the induction of column axial loads associated with the lateral load is assumed to be negligible. The reason for this is that: (1) Q is typically small in magnitude compared to the applied gravity loads in frame stability analysis, which means P will not change significantly relative to its original value; and (2) Q will induce varying magnitudes compressive and tensile forces in the columns, all of which sum to zero in the vertical direction, resulting in some columns having increased lateral stiffness while others will experience a reduction. In other words, the compressive and tensile forces in the columns will both decrease and increase the lateral stiffness, respectively, resulting in insignificant changes to the overall lateral stiffness of the frame. In reality, the induction of lateral loads will not always have a negligible effect on the total lateral stiffness of the frame if the material is stressed in the non-linear range, in which case the stiffness in the column can simply be calibrated based on the actual axial load.

Let the subscripts i and j correspond to the indices of the columns and beams, respectively, from left to right.

$$\sum_{i=1}^{n+1} Q_i = Q \tag{5}$$

By equilibrium of forces, the axial forces in the beams of the frame, $N_{b,j}$, are shown in Fig. (2) and expressed generally in Eq. (6).

$$N_{b,j} = Q - \sum_{k=1}^{j} Q_k; \quad j = \{1,2,...,n\} \tag{6}$$

Tension-only lateral bracing is supplied to each column with stiffness $S_{L,i}$, and is assumed to deform with the upper ends of each column. Let the axial stiffness of each beam be denoted as $S_{b,j}$ in Eq. (7).

$$S_{b,j} = E_{b,j} A_{b,j} / L_{b,j}; \quad j = \{1,2,...,n\} \tag{7}$$

Where $E_{b,j}$, $A_{b,j}$ and $L_{b,j}$ are the elastic modulus, cross-sectional area and length of beam j, respectively. The difference between the lateral displacements of adjacent columns is affected by the stiffness of the beam in between via Eq. (8).

$$\Delta_{i+1} - \Delta_i = \left(Q - \sum_{k=1}^{i} Q_k \right) / S_{b,i}; \quad i = \{1,2,...,n\} \tag{8}$$

Based on the method derived in [6], the lateral stiffness of each column, $S_{c,i}$, can be calculated via Eq. (3). By Hooke's law, the upper-end lateral deflection of each column, Δ_i, is given via Eq. (9).

$$\Delta_i = Q_i / (S_{c,i} + S_{L,i}); \quad i = \{1,2,...,n+1\} \tag{9}$$

3.1 Lateral Deflections of Columns

The lateral deflections, Δ_i, and distributed lateral loads, Q_i, of each column can be expressed as a function of Q and the stiffnesses S_L, S_c and S_b, by solving the system of $2n$+2 equations comprised of Eqs. (5), (8) and (9), which are all linear in Δ_i and Q_i. The resulting solution will vary depending on the number of columns in the frame, but can always be expressed in the form of Eqs. (10). By using Eqs. (10), the upper-end displacement of each column as a result of the lateral force Q can be evaluated.

$$\Delta_i = \frac{Q}{S_{eq,i}} \tag{10a}$$

$$S_{eq,i} = \frac{S_{NUM}}{S_{DEN,i}} \tag{10b}$$

where $S_{eq,i}$ is the effective lateral stiffness of the column as a result of the lateral load being applied on the left-most column, obtained by solving Eqs. (5), (8) and (9). It will be shown in the following text that the numerator S_{NUM} is an indicator of the stability in the frame whereas the denominator $S_{DEN,i}$ relates to the

relative deformations of the columns. As such, S_{NUM} can be called the stability-related stiffness product, while S_{DEN} is called the deformation-related stiffness product. As an example, the solution to Eqs. (5), (8) and (9) for an n = 1 bay frame is given in Eqs. (11).

$$\Delta_1 = Q\left(\frac{S_{b,1} + (S_{c,2} + S_{L,2})}{(S_{c,1} + S_{L,1})(S_{c,2} + S_{L,2}) + S_{b,1}(S_{c,1} + S_{L,1}) + S_{b,1}(S_{c,2} + S_{L,2})}\right) = Q\left(\frac{S_{DEN,1}}{S_{NUM}}\right) \quad (11a)$$

$$\Delta_2 = Q\left(\frac{S_{b,1}}{(S_{c,1} + S_{L,1})(S_{c,2} + S_{L,2}) + S_{b,1}(S_{c,1} + S_{L,1}) + S_{b,1}(S_{c,2} + S_{L,2})}\right) = Q\left(\frac{S_{DEN,2}}{S_{NUM}}\right) \quad (11b)$$

Where Δ_1 is the lateral deflection of the first column and Δ_2 is the lateral deflection of the second column when Q is applied on the first column. It is important to note, however, the deflection also depends on the location of Q. If Q is instead applied to the second column instead of the first, then the deflections take the form of Eqs. (12).

$$\Delta_1 = Q\left(\frac{S_{b,1}}{(S_{c,1} + S_{L,1})(S_{c,2} + S_{L,2}) + S_{b,1}(S_{c,1} + S_{L,1}) + S_{b,1}(S_{c,2} + S_{L,2})}\right) = Q\left(\frac{S_{DEN,1}}{S_{NUM}}\right) \quad (12a)$$

$$\Delta_2 = Q\left(\frac{S_{b,1} + (S_{c,1} + S_{L,1})}{(S_{c,1} + S_{L,1})(S_{c,2} + S_{L,2}) + S_{b,1}(S_{c,1} + S_{L,1}) + S_{b,1}(S_{c,2} + S_{L,2})}\right) = Q\left(\frac{S_{DEN,2}}{S_{NUM}}\right) \quad (12b)$$

First, the value of S_{NUM} is identical for all columns regardless of the location of the lateral load, and as such, does not have the index i. It is then noted that the instability of the frame occurs for all columns when S_{NUM} diminishes to zero, resulting in $S_{eq,i} = 0$ and $\Delta = \infty$. Note that Q does not have to be present for instability to occur since an infinitesimally small value of Q would still result in $\Delta_i = \infty$ if $S_{eq,i} = 0$. On the other hand, $S_{DEN,i}$ varies between the columns and relates to the relative magnitudes of deflections experienced by each column. In fact, as shown between Eqs. (11) and (12), if Q is applied on a different column, the axial forces in the beams in Fig. 2 and the values of $S_{DEN,i}$ will change. The lateral deflection of the column where Q is directly applied will always be greater than the deflections of the other columns, with the deflections decreasing further away from the location of Q because of the axial deformation of beams. In other words, one can visualize that the further away a column is from the lateral load, the less it will deflect since the beams in between the column and the load act as springs in series. As such, if Q is applied on one end of the frame, the column on the opposite end of the frame will deflect by the least

amount. The lateral deflection on the far side of an *n*-bay frame is quantified via Eq. (13), which is a special case whereby S_{DEN} is the product sum of the beam stiffnesses.

$$\Delta_{n+1} = Q\left[\prod_{j=1}^{n} S_{b,j}\right] / S_{NUM} \tag{13}$$

Lateral deflections of the intermediate columns cannot be expressed in simple terms but are readily obtainable by solving the linear system of equations in Eqs. (5), (8) and (9). The deflections of the intermediate columns gradually decrease towards the end of the frame furthest away from the column on which Q is applied.

3.2 Lateral Deflection and Stability of the Frame

To determine the lateral deflection and stability of a frame such as the one in Fig. (2), an equivalent, simplified approach for calculating $S_{eq,i}$ is presented. The method used to determine $S_{eq,i}$ involves applying the equivalent spring stiffness concept [18]. In doing so, the frame shown in Fig. (2) is decomposed into a system of springs in parallel and in series, as shown in Fig. (3).

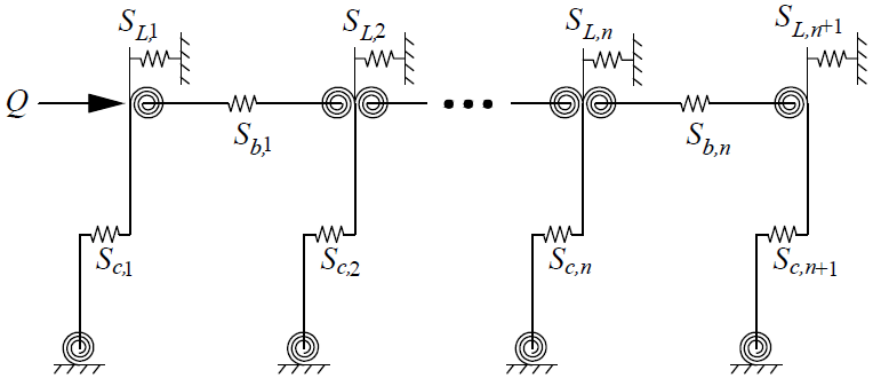

Figure 3 – Equivalent spring system for the storey frame in Fig. (2)

The equivalent spring stiffness of the storey is evaluated by continually replacing pairs of springs with single springs of equivalent stiffness starting from the right end of the frame and moving towards the left end, where Q is applied. Note that a similar analysis can be done with Q applied on the upper end of a different column, as long as $S_{eq,i}$ is calculated for the column on which Q is applied. Doing so may result in a different value of $S_{eq,i}$ when the frame is stable, but not during instability which corresponds to $S_{eq,i}$ =

0 occurring simultaneously for all columns and is entirely independent of whether Q is present in the analysis. For the purpose of this paper, the tilde symbol, '~', is hereby used to denote the series spring stiffness operation shown in Eq. (14).

$$S_1 \sim S_2 = \left[1/S_1 + 1/S_2 \right]^{-1} \tag{14}$$

The equivalent stiffness of a system of springs in series can be calculated using the operation in Eq. (14) in which the total displacement experienced by the springs is equal to the sum of displacements experienced by the two springs in the system. Note that this operation is commutative and associative but not distributive, as expressed via Eqs. (15) below.

$$S_1 \sim S_2 = S_2 \sim S_1 \tag{15a}$$

$$(S_1 \sim S_2) \sim S_3 = S_1 \sim (S_2 \sim S_3) \tag{15b}$$

$$S_1 \sim (S_2 + S_3) \neq S_1 \sim S_2 + S_1 \sim S_3 \tag{15c}$$

Conversely, stiffnesses are additive if springs are arranged in parallel, whereby the two springs deform by the same distance. To demonstrate the proposed approach, Fig. (3) is repeated in Fig. (4) but in its deformed state. Note that the upper-end column displacements closest to the applied load are purposely shown to be greater than those furthest away, to reflect how a system with axially deforming beams would normally behave. It is also noted that the contribution of other non-structural elements such as cladding to the lateral stiffness of the system is neglected in the proposed method as these cannot be relied upon for structural integrity. Such an assumption is also conservative with regards to stability analysis.

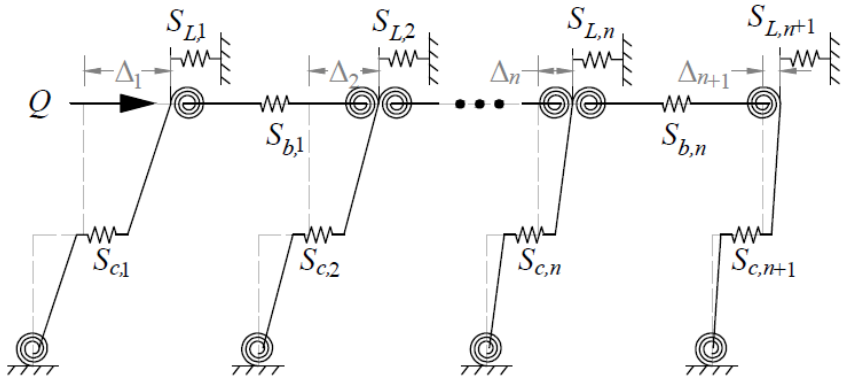

Figure 4 – Deformed state of the equivalent spring system in Fig. (3)

Starting at the right end of the frame in Fig. (4), the right-most column deforms in parallel with the upper end of the brace connected at its upper end (with the same deflection of Δ_{n+1}). The equivalent lateral stiffness of this column-brace system is therefore the sum of the lateral stiffness of the column and the brace, shown via the equivalent spring in Fig. (5).

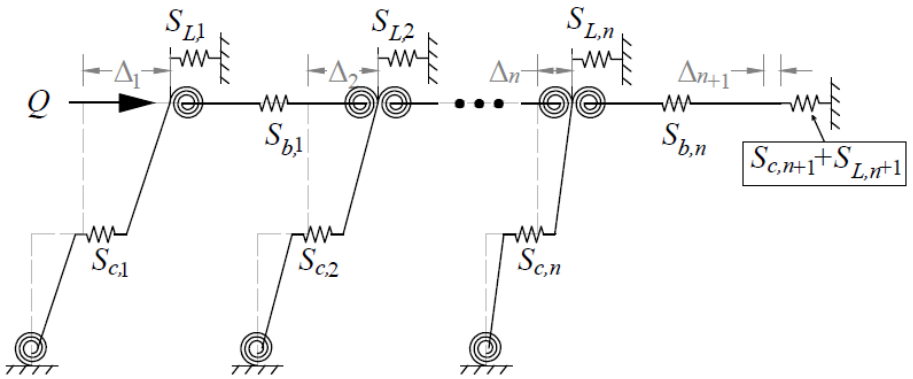

Figure 5 – Replacing a column and its brace in parallel with an equivalent spring

Then, the beam connected to this column (beam n) deforms by $(\Delta_n - \Delta_{n+1})$. As such, the $(n+1)^{th}$ column-brace system acts in series with the end beam, since the sum of their displacements is equal to the displacement experienced at the left end of beam n, Δ_n. The equivalent spring stiffness of this beam-column-brace system is therefore obtained by using the operator in Eq. (14) on the lateral stiffness of the beam. The equivalent spring stiffness of this system is shown in Fig. (6), and is attached to the upper end of column n.

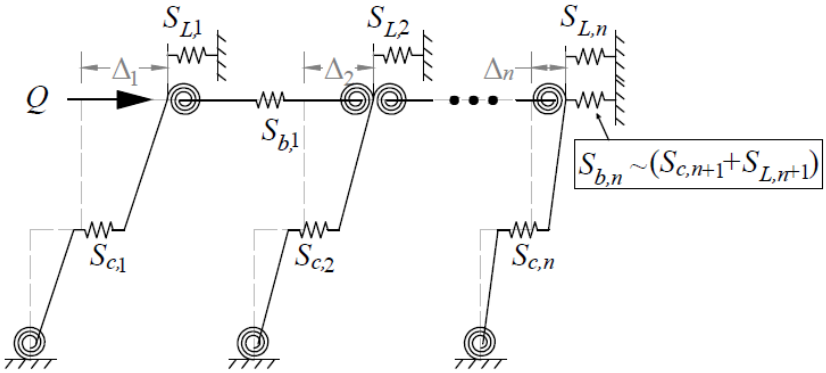

Figure 6 – Replacing a beam and column-brace system in series with an equivalent spring

This resulting system acts in parallel with the n^{th} column-brace system, which together acts in series with beam n-1, and so forth. The process of calculating the equivalent lateral stiffness in each step and replacing the springs is repeated until the equivalent stiffness of all of the members of the storey (the last one being Column 1) is lumped into a single effective value, $S_{eq,1}$, shown in Fig. (7).

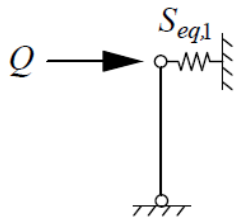

Figure 7 – Using an equivalent spring stiffness, $S_{eq,1}$, to represent the entire storey frame

By doing this, $S_{eq,1}$ can generally be expressed via Eq. (16).

$$S_{eq,1} = \left[\left\{\left[(S_{c,n+1} + S_{L,n+1}) \sim S_{b,n} + S_{c,n} + S_{L,n}\right] \sim S_{b,n-1} + S_{c,n-1} + S_{L,n-1}\right\} \sim \ldots \sim S_{b,1} + S_{c,1} + S_{L,1}\right] \quad (16)$$

As seen in Eq. (16), it is difficult to write the equivalent lateral stiffness as an equation. Rather, the equivalent pseudo-algorithm in Fig. (8) is relatively easier to understand and implement.

$S_{eq,1} = S_{c,n+1} + S_{L,n+1}$
for $j = n$ *to* 1
    $S_{eq,1} = S_{eq,1} \sim S_{b,j}$
    $S_{eq,1} = S_{eq,1} + S_{c,j} + S_{L,j}$
return $S_{eq,1}$

Figure 8 – Pseudo-algorithm for calculating equivalent spring stiffness

Fig. (8) is applicable for calculating equivalent stiffness of the frame $S_{eq,1}$ corresponding to the application of a lateral load at Column 1. If Q is applied to a different column then the same concept can be used to replace the members starting from both ends of the frame with equivalent springs and moving towards the location of application of Q until only one spring remains with stiffness $S_{eq,i}$. The value of $S_{eq,i}$ obtained via the proposed method can therefore be used to determine the maximum lateral deflection of a frame at the column upon which Q is applied via Eq. (10a).

311 In terms of stability, as demonstrated previously, S_{NUM} is independent of the location of Q and is the same
312 for all columns. All of the columns will reach $S_{eq,i} = 0$ simultaneously during buckling. As such, the storey
313 frame will become unstable when the effective lateral stiffness of any column, $S_{eq,i}$, is calculated to be
314 zero. Rather than solving the system of equations in Eqs. (5), (8) and (9), $S_{eq,i}$ can be determined using the
315 equivalent spring stiffness approach in Fig. (8). Moreover, the order in which the springs are decomposed
316 does not matter since $S_{eq,i} = 0$ for all columns. Thus, as long as an expression of $S_{eq,i}$ for any column, say
317 Column 1 via $S_{eq,1}$, can be formulated, then critical axial loads of the frame can be determined by solving
318 for the values of P_i that result in $S_{eq,1} = 0$. As the lateral stiffness of a column monotonically decreases
319 with increasing axial load, $S_{eq,1}$ will also monotonically decrease as loads on the frame are increased. As
320 such, the Newton-Raphson method [34] can be used to determine the critical gravity loads of the frame
321 via root-finding.
322 Note that in both the lateral deflection and stability analyses, if tension-only lateral bracing exists, some
323 braces may only provide lateral stiffness for a certain direction. That is, if sway occurs towards the left,
324 then only the braces oriented towards the left direction will be effective. Similarly, if sway occurs towards
325 the right, then only the braces oriented towards the right direction will be effective. The amount of lateral
326 bracing in either direction may vary in some cases. Note that tension-only bracing is a limitation to the
327 proposed method. The method can be extended towards tension-compression bracing but the
328 consideration of flexural buckling of a bracing member on the results of the proposed method remains to
329 be investigated. As such, the analysis procedure shown in Fig. (8) may need to be performed with
330 assuming lateral deflection or sway buckling in both directions separately. For stability analysis, the
331 critical gravity load will be taken as the minimum load causing instability from either case. Additionally,
332 it is assumed that the frame buckling precludes component buckling. Furthermore, as discussed in [5], the
333 axial load of each column is bounded by $P_{u,i}$, which is the rotational buckling load shown in Eq. (17).

334 $$P_u = \frac{\pi^2 EI}{(KL)^2} \tag{17}$$

When $P = P_u$, the denominator of lateral stiffness for the individual column obtained in Eq. (3) becomes zero and the individual column buckles rotationally. The effective length, KL, of the column corresponds to the rotational buckling mode and K can be approximated within 4% for semi-rigidly connected column via Eq. (18) in [35,36].

$$K \approx \sqrt{\frac{\left(\pi^2 + (6-\pi^2)r_u\right)\times\left(\pi^2 + (6-\pi^2)r_l\right)}{\left(\pi^2 + (12-\pi^2)r_u\right)\times\left(\pi^2 + (12-\pi^2)r_l\right)}} \tag{18}$$

Alternatively, an exact value of P_u can be obtained using root finding methods whereby the denominator of β in Eq. (4) is set to zero. The minimum positive value of P_u satisfying this condition is the rotational buckling load. The same limitation is imposed for the use of the proposed method, since it makes use of the lateral stiffness equation in [6].

As the concept of column effectiveness is established based on the assumption that the columns behave elastically, the results obtained in Eq. (17) may not typically agree with experimental results if the column experiences inelastic flexural buckling. The tangent modulus method may alternatively be applied to account for the inelastic buckling of columns which occurs in reality, as demonstrated in [16]. In doing so, the effective value of E may be approximated using applicable empirical equations, such as the one proposed by Yura & Helwig [37] in Eq. (19), as necessary.

$$E = E_0 \tau \tag{19a}$$

$$\tau = \begin{cases} -7.39\dfrac{P}{P_y}\log_{10}\left(\dfrac{P}{0.85P_y}\right); & \dfrac{P}{P_y} \le \dfrac{1}{3} \\ 1; \quad \text{otherwise} \end{cases} \tag{19b}$$

Where E_0 = 200 GPa and P_y is the product of cross-sectional area and yield stress, f_y. In such a case, the value of E can be conservatively reduced by the empirical τ factor proposed when solving for the critical inelastic buckling load. Finally, it is noted that the proposed method assumes that the beams are laterally braced (otherwise, lateral-torsional buckling can occur) and that the members consist of compact sections not subjected to local buckling.

3.3 Behaviour of the Series Spring Stiffness Operator

Note that identity in Eq. (20), which indicates that Eq. (14) always reduces the stiffness below the minimum of the individual stiffnesses if both the inputs S_1 and S_2 are positive values. The exception to this is that if either of the values is infinity, say $S_2 = \infty$, then $S_1 \sim S_2 = S_1$, resulting in no reduction to S_1. Such a case would apply when calculating the equivalent lateral stiffness of a column connected to a rigid beam.

$$S_1 \sim S_2 \leq \min\{S_1, S_2\}; \quad S_1 > 0, \quad S_2 > 0 \tag{20}$$

In the case of the frames being analyzed in this application, columns act as springs in series with beams, which means that if the column lateral stiffness is negative, one of the variables in the operation (S_1 or S_2) can be negative. In the physical sense, negative column spring stiffness can be thought of as a deficit in the lateral stiffness imposed on the rest of the frame to provide in order to maintain stability. Logically, this deficit should increase if the column is attached to a beam that is considered to deform axially compared to when the beam is considered to be rigid.

A beam-and-column system acting in series is now considered, with the lateral stiffness of the column being S_c and the lateral stiffness of the beam being S_b. It is possible that S_c is negative if the column is loaded in compression, while $S_b = EA/L$ is always positive. By observing Eq. (14), if S_c is negative and equal in magnitude to S_b, then the equivalent lateral stiffness $S_c \sim S_b$ is undefined. To explain this phenomenon, knowing that S_c is initially greater or equal to zero in the absence of loading and decreases as the load increases [5], it can be seen that when S_c is negative and the magnitude of S_c approaches S_b, the result $S_c \sim S_b$, or the effective lateral stiffness of the beam-and-column system, approaches negative infinity. This relation is expressed in Eq. (21).

$$\lim_{|S_c| \to S_b} S_c \sim S_b = -\infty; \quad S_c < 0, \quad S_b > 0 \tag{21}$$

With this in mind, one can conclude that if S_c is negative, then instability must occur before the magnitude of S_c exceeds S_b. Thus, in general, if one of the values S_1 or S_2 in Eq. (14) is negative, it is not possible in this application for the magnitude of the negative value to exceed that of the positive value. As such, the domain of applicability for Eq. (14) can be expressed in Eq. (22).

$$|\min\{S_1, S_2\}| \leq \max\{S_1, S_2\} \tag{22}$$

It can be shown that within the extended domain in Eq. (21), the identity in Eq. (18) still applies. Thus, Eq. (23) is extended as follows.

$$S_1 \sim S_2 \leq \min\{S_1, S_2\}; \quad |\min\{S_1, S_2\}| \leq \max\{S_1, S_2\} \tag{23}$$

Therefore, for the application of the proposed equivalent spring stiffness operator in Eq. (14) towards storey-based stability, it is demonstrated that the resulting equivalent series stiffness will always be less than or equal to the minimum of the stiffness terms in the operation. As a corollary, the consideration of axial beam deformations in a storey frame will always reduce its lateral stiffness compared to when the axial beam deformations are neglected via the assumption of a rigid floor or roof system. It is also worth mentioning that the reciprocal series stiffness function in Eq. (14) is performed the same number of times as the number of bays in the frame via the procedure shown in Fig. (8). In other words, adding more bays has the effect of adding more springs in series. In general, the wider a frame is (that is, as the number of beams in the frame increases, or the length of the beams increases and thus reduces *EA/L*), the more significant the reduction to the lateral stiffness will become as a result of considering beam axial deformations.

3.4 Local Stiffness Reduction Factor

Let ς be defined as the ratio of the stiffness of a beam S_b to the stiffness of a directly connected column-brace system (S_c + S_L) acting in series with S_b (either to the left or right) in Eq. (24).

$$\varsigma = S_b / (S_c + S_L) \tag{24}$$

Then it can be shown via substitution into Eq. (14) that the equivalent stiffness of this local system is equal to $\varsigma/(1+\varsigma)$ times the stiffness of the adjacent column-brace system. As such, the consideration of beam axial deformations results in a reduction factor of $\varsigma/(1+\varsigma)$ to the lateral stiffness of the local system. The reduction factor can thus be used to estimate the relative effect of beam axial deformations on the lateral stiffness of a frame, and is plotted in Fig. (9). However, it should be understood that the actual reduction to the lateral stiffness of the frame involves taking the series equivalent stiffness of S_b with an

equivalent spring system potentially comprised of many members, rather than just that of the immediately connected column-brace system. Nevertheless, it is demonstrated in the following numerical examples that if ς is sufficiently large for all beams, then the effect of beam axial deformations on the critical gravity load of the frame is negligible.

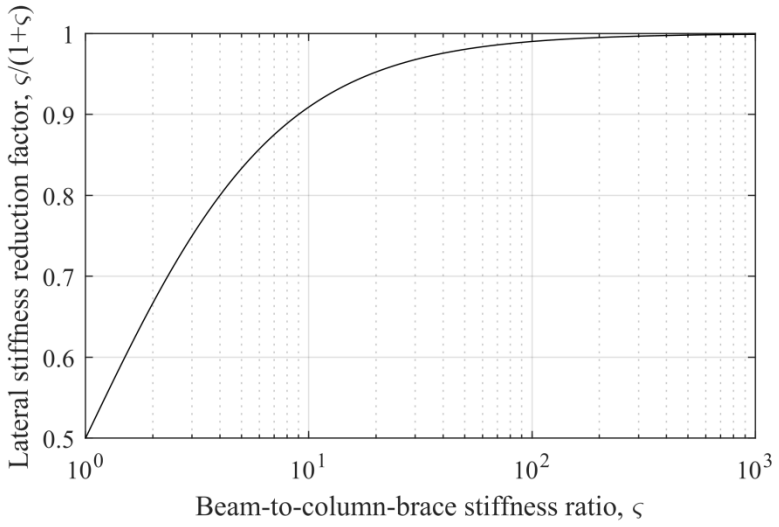

Figure 9 – Lateral stiffness reduction factor versus beam-to-column-brace stiffness ratio

However, if for any beam ς is small– say in the order of 10^1 – then beam axial deformations will have a much greater effect on the frame lateral stiffness and should not be ignored. Thus, the minimum value of ς in the frame can be used as an indicator to predict the significance of the effect of the beam axial deformations on its lateral stiffness. It is also noted that if the column lateral stiffness becomes negative (i.e. it relies on the other columns in the frame to maintain stability) then ς will become negative, and the relative effect of beam axial deformations on the lateral stiffness of the system in such a case is comparable to that of when ς is positive but the same magnitude for sufficiently large $|\varsigma|$. Moreover, when finding the minimum value of $|\varsigma|$ in a frame, the values of ς for each beam should be evaluated considering both columns connected on the left and right ends of the beams.

4 Numerical Examples

The application of the proposed method is demonstrated for three numerical examples. The frames are loaded proportionally, and the critical gravity load corresponding to the instability of the frame is

calculated using the proposed method. That is, the Newton-Raphson method [34] was used to determine the gravity load resulting in $S_{eq,1} = 0$. The results are also compared with the critical gravity loads obtained via the Xu & Liu [6] equation, which neglects the effects of beam axial deformations on the storey-based lateral stiffness. Note that rather than using the Taylor series approximation to estimate the critical gravity load as suggested in [6], the exact solution was obtained in the examples by setting Eq. (3) to zero via the Newton-Raphson method [34].

4.1 Example 1

The first example is a proportionally loaded semi-braced four-bay frame adapted from [35] and originally sourced from [37] and shown in Fig. (10).. The beam-to-column connections are pinned ($r_L = r_R = 0$ for all beams, $r_u = 0$ for all columns), the interior columns are fixed to the ground ($r_l = 1$), and the exterior columns are pinned to the ground ($r_l = 0$). The exterior columns are therefore lean-on and rely on the lateral stiffness provided by the interior columns and/or lateral bracing in order to maintain stability and sustain the applied gravity loads.

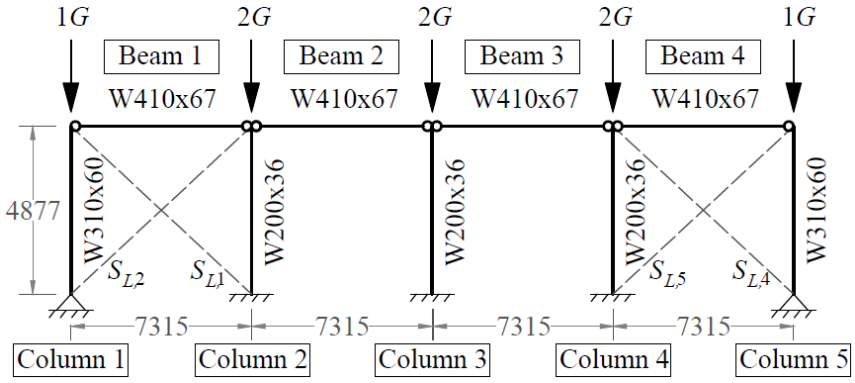

Figure 10 – Four-bay frame subjected to proportional gravity loading

Diagonal bracing of magnitude S_L, varying from zero to 10000 kN/m is provided at each of the exterior bays and are assumed to be tension-only in the investigation. Note that the maximum value of 10000 kN/m can be provided by a 28 mm diameter bar via Eq. (25) [6].

$$S_L = \frac{E_L A_L}{L_L} \cos^2 \theta_L \tag{25}$$

Where the subscript L refers to the diagonal tension-only brace and θ is its angle from the horizontal. As such, if sway occurs in the right direction then $S_{L,2} = S_{L,5} = S_L$ and $S_{L,1} = S_{L,4} = 0$. Conversely, if sway occurs in the left direction then $S_{L,1} = S_{L,4} = S_L$ and $S_{L,2} = S_{L,5} = 0$. Although the critical gravity load will be the minimum of the critical gravity loads obtained in the sway analysis of both directions separately, the frame is symmetrical so both directions will yield the same results. The lengths of the members are shown in Fig. (10). The moments of inertia and cross-sectional areas of the beams are $I_b = 245\times10^6$ mm^4 and $A_b = 8580$ mm^2, respectively. For the exterior columns, $I_{c,1} = I_{c,5} = 129\times10^6$ mm^4 and $A_{c,1} = A_{c,5} = 7610$ mm^2. For the interior columns, $I_{c,2} = I_{c,3} = I_{c,4} = 34.1\times10^6$ mm^4 and $A_{c,2} = A_{c,3} = A_{c,4} = 4570$ mm^2. The slenderness ratios of the interior and exterior members are 39.5 and 37.5, respectively. As such, the columns will buckle inelastically at high loading levels. To account for this, the tangent modulus method proposed in [37] is used to adjust the elastic modulus according to Eq. (26) at high loading levels.

$$E = E_0 \tau \tag{26a}$$

$$\tau = \begin{cases} -7.39\dfrac{P}{Af_y}\log_{10}\left(\dfrac{P}{0.85Af_y}\right) \geq 0; & \dfrac{P}{Af_y} \geq \dfrac{1}{3} \\ 1.0; \quad \text{otherwise} \end{cases} \tag{26b}$$

Where $E_0 = 200$ GPa and $f_y = 350$ MPa are the elastic modulus and yield stress of the steel, respectively. The critical gravity load, G_{cr}, corresponding to the instability of the frame, was obtained with and without considering the effects of beam axial deformations and shown in Fig. (11) for varying amounts of the diagonal bracing, S_L. Note that the analysis for this example is independent of the assumed values of v_{FN} since the beams are simply supported (in Eq. (2), v_{FN} is multiplied by $r_F = 0$). From Fig. (11) it can be seen that there is virtually no difference in this example between the critical gravity loads obtained with and without considering the effects of beam axial deformations. As the amount of lateral bracing increases, the critical gravity load increases from the unbraced case ($G_{cr} = 278$ kN) towards the fully-braced case ($G_{cr} = 624$ kN). The value of $G_{cr} = 278$ kN corresponding to the unbraced case matches the value reported in the original example [35]. Note that the critical gravity load in the fully-braced case corresponds to the imminent rotational buckling of the interior columns ($G_{cr} \approx G_u = 624$ kN). A maximum

difference between the two curves of 0.024% occurs at $S_L = 4.54\times10^2 = 454$ kN/m, with a reduction to the critical gravity load of only 134 N when beam axial deformations are considered. The reason for the trivial difference is explained in the following paragraph.

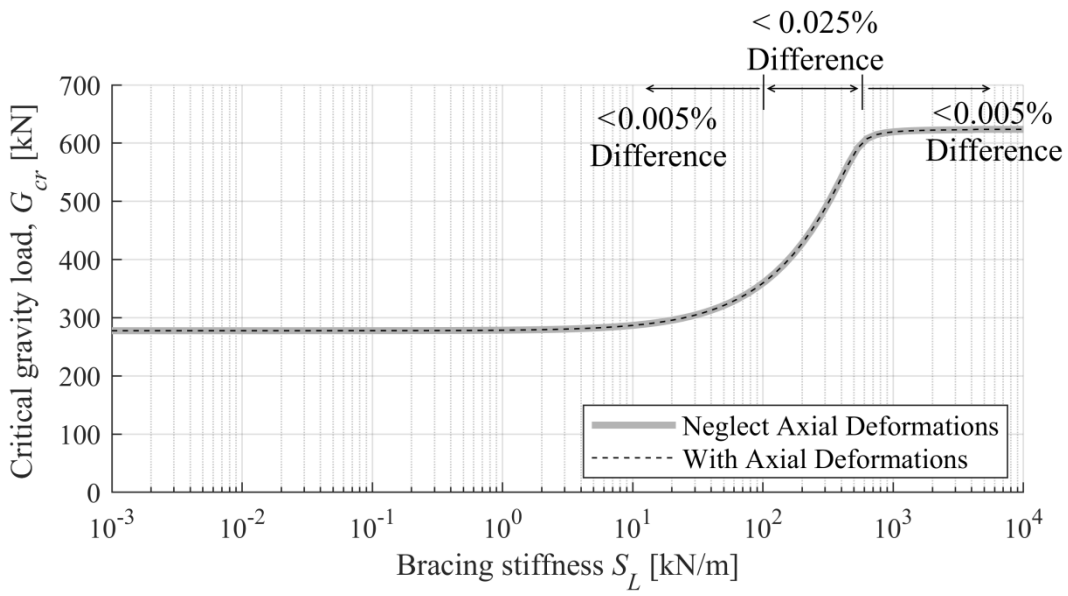

Figure 11 – Critical gravity load of four-bay frame with varying lateral bracing stiffness

The first-order elastic lateral stiffness is the lateral stiffness of a column in the absence of the effect of axial loading ($P_i = 0$). For the exterior columns, the first-order lateral stiffness is zero since the columns are lean-on. For the interior columns, the first-order lateral stiffness is 176 kN/m. However $S_b = 2.35\times10^5$ kN/m for all beams, which is $\varsigma = 1335$ times the stiffness of the interior columns in the absence of bracing and loading via Eq. (24), and $\varsigma = \infty$ times the stiffness of the exterior columns in the absence of bracing and loading. Although ς will change as loading of the columns begins to occur, using the value of ς considering just the first-order lateral stiffness will provide a conservative prediction of the effect of beam axial deformations on the critical gravity load. This is because ς will generally increase as the lateral stiffnesses of the columns are decreased with gravity loading. As such, even the minimum value of the local stiffness reduction factor, $\varsigma/(1+\varsigma)$, achieved using $\varsigma = 1335$, is very close to unity (0.9993). As such, the reduction of the lateral stiffness of the frame accounting for beam axial deformations will be

negligible in the absence of bracing. In fact, the difference in critical gravity loads is only 0.014 kN (0.005%) for $S_L = 0$.

Now, as the lateral stiffness of the bracing is increased, the value of ς in Eq. (24) will be reduced, and it would follow that the effect of beam axial deformations increases as S_L increases. However, as the lateral bracing increases past 500 kN/m in Fig. (5), the critical gravity load asymptotically approaches the rotational buckling load, $G_u = 624$ kN. The imminent rotational buckling of the interior columns thus governs the failure of the frame for high values of S_L, and for design purposes the frame can be treated as being fully braced. The rotational buckling loads of the columns are neither functions of the axial nor flexural stiffness of the connecting beams. As such, the difference between the critical gravity load with and without considering beam axial deformations becomes less significant as the critical gravity loads approach the rotational buckling load (for $S_L > 454$ kN/m). Thus even at $S_L = 10^4 = 10000$ kN/m, despite the resulting low minimum value of $\varsigma = 23$ in the frame, the difference in critical gravity loads with and without considering the effects of beam axial deformations is negligible due to the imminence of rotational buckling occurring at the critical gravity load. Note, however, that with $\varsigma = 23$, the lateral stiffness of the frame will be significantly reduced for loads below the rotational buckling load. For instance, the first-order lateral stiffness of the entire frame with $S_L = 10000$ kN/m is 20530 kN/m with neglecting beam axial deformations, but is reduced to 17880 kN/m when beam axial deformations are considered (a 13% decrease). In any case, the maximum difference of 0.024% between critical gravity loads with and without consideration of beam axial deformations thus occurs at an intermediate value of $S_L = 454$ kN/m whereby the value of ς is relatively low and the rotational buckling load is not imminent ($G_{cr} = 543$ kN $\ll G_u$). Note that this intermediate value of bracing stiffness corresponds to the semi-braced case for the frame, since the critical gravity loads are well within the limiting values corresponding to the unbraced and fully-braced cases. The lateral stiffness of 454 kN/m is comparable to that which would be provided by 6 mm tension cables at each of the locations shown in Fig. (10).

A finite element analysis (FEA) was conducted via ABAQUS [38] to verify the theoretical accuracy of the critical gravity loads of the frame obtained via the proposed method for the cases with $S_L = 0.0$ kN/m

(unbraced), S_L = 454 kN/m (semi-braced), and S_L = 10000 kN/m (fully-braced). Note that S_L = 454 kN/m corresponds to the maximum difference of 0.024% between the critical gravity loads obtained from considering and neglecting the axial beam deformations in this example. Cubic Euler-Bernoulli beam elements (B23), which neglect shear deformations, were used in all members in the model shown in Figs. (12). Figs. (12) show screen captures of the finite element model produced in the ABAQUS [38] user interface, which include annotations in grey for the purpose of clarity. To simulate the effect of neglecting the beam axial deformations, the linking interaction constraint shown in Fig. (12a), which restrains the lateral displacement of the adjacent column upper-end nodes to be equal, was toggled on. To realize the effect of the beam axial deformations, the linking constraint was toggled off. The analysis is identical regardless of whether the sway direction is to the right or to the left. As such, the diagonal braces were modelled via Cartesian springs on the upper ends of Columns 2 and 5 in the horizontal direction (simulating sway to the right) shown in Fig. (12b), with the value of the spring stiffness equal to S_L. The Cartesian springs provide user-specified values of lateral stiffness against the horizontal translation of the respective nodes. Note that the use of Cartesian springs was found to be equivalent to the direct modelling of the diagonal axial members, but the latter case was prone to convergence errors in ABAQUS [38]. Finally, the Join + Rotation connector section shown in Fig. (12c) was used to join the ends of the members (particularly, the ends of connecting columns and beams) via pin connections (free rotation and joined translation).

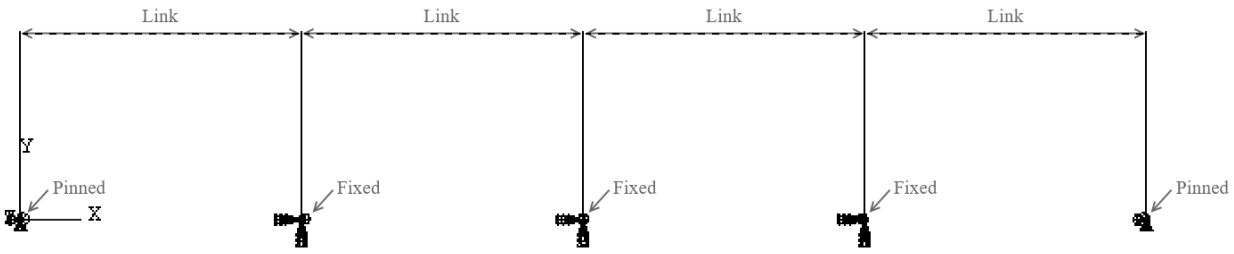

Figure 12(a) – Linking Constraints in FEA Model for Theoretical Validation of Example 1

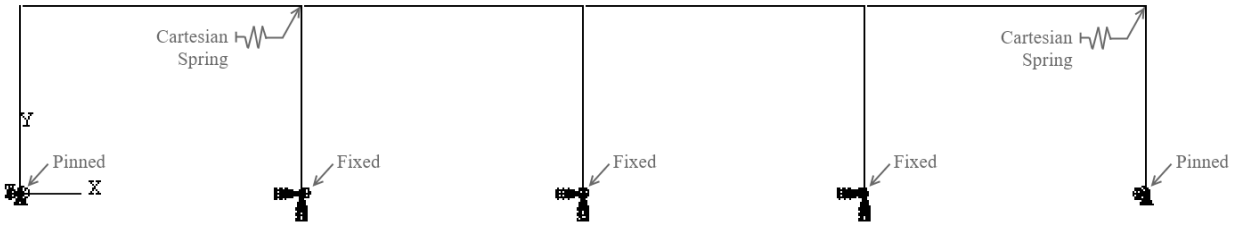

532

533 **Figure 12(b) – Bracing Constraints in FEA Model for Theoretical Validation of Example 1**

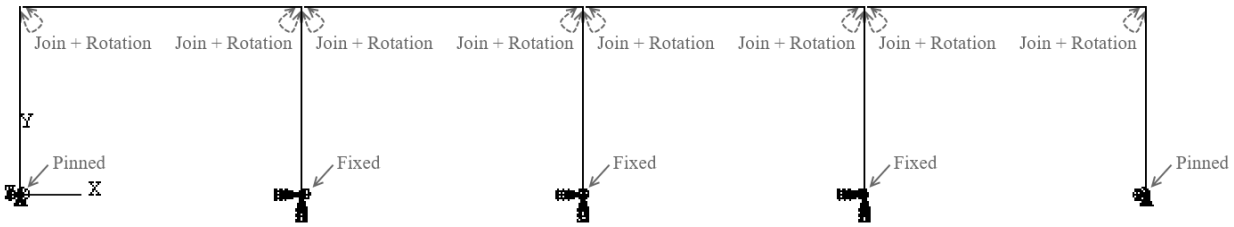

534

535 **Figure 12(c) – Joining Constraints in FEA Model for Theoretical Validation of Example 1**

536 The elastic moduli of the members in the model were calculated using Eq. (26). The sway buckling load
537 of the frame obtained from FEA analysis was found to be virtually exact to the results of the example. In
538 terms of the validation of the FEA model itself, a verification package has been provided by ABAQUS
539 [38] whereby the elements used in the current study have been verified against a variety of validation
540 examples. Additionally, the use of the finite element analysis procedure in ABAQUS [15-16,20] or other
541 similar finite element software [12,14] has commonly been adopted for the purposes of validation in
542 previous storey-based stability methods. The results of the critical gravity loads, G_{cr}, are shown in Table 1,
543 obtained using the Xu & Liu [6] storey-based stability method neglecting the axial beam deformations,
544 the proposed storey-based stability method considering the axial beam deformations, and FEA with and
545 without toggling the linking constraint.

546 **Table 1. Validation of critical gravity loads, G_{cr} (kN), obtained from proposed method using FEA**
547 **for Example 1**

Calculation Method	Xu & Liu [6]	FEA	Proposed Method	FEA
Considers axial beam deformations?	No	No	Yes	Yes
S_L = 0.0 kN/m	277.317	277.317	277.303	277.303
S_L = 454 kN/m	564.507	564.506	564.372	564.372
S_L = 10,000 kN/m	623.427	623.428	623.422	623.423

548

As seen from Table 1, the differences between the results of the critical gravity loads obtained between the storey-based stability methods and FEA are at most 0.001 kN (0.004%). Therefore, the proposed method is shown to be virtually exact to the theoretical governing Euler-Bernoulli equation. The buckled shapes of the frame obtained from the FEA model for each case are also shown in Figs. (13).

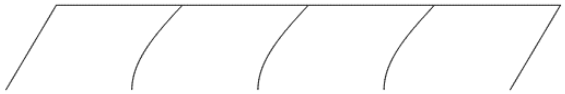

Figure 13(a) – Buckled shape of the four-bay frame with S_L = 0 kN/m (unbraced)

Figure 13(b) – Buckled shape of the four-bay frame with S_L = 454 kN/m (semi-braced)

Figure 13(c) – Buckled shape of the four-bay frame with S_L = 10000 kN/m (fully-braced)

It is clear from observing Figs. (13) that the lateral sway mode governs the buckling for the first two cases ($S_L \leq 454$ kN/m), indicated by the large lateral deflections of the columns in the buckled shapes. For S_L = 10000 kN/m, Fig. (13c) confirms that the simultaneous rotational buckling of the interior columns is imminent during the critical gravity load of G_{cr} = 623.4 kN ≈ G_u = 624 kN. This is apparent by noting that the deflections of the upper ends of the columns are small compared to mid-height deflections of the interior columns. In general, as the amount of lateral bracing increases, the curvature experienced by the individual columns relative to the magnitude of lateral sway in the buckled shape increases.

4.2 Example 2

The effects of varying the number of bays and the beam axial stiffness are investigated in this numerical example. This example is adapted from a similar study by Ma & Xu [16] who studied the effects of shear deformations on the stability of unbraced steel frames with lean-on columns. Consider the *n*-bay lean-on system in Fig. (14) consisting of a cantilever column which supports *n* lean-on columns. As such, r_u = 0 and r_l = 0 for all columns except r_l = 1 for the cantilever and the flexural stiffness of the beams have no

effect on lateral stiffness of the columns. For the reason of simplicity, all of the columns have the same cross-sectional properties (I_c = 8600×10^6 mm^4, A_c = 74300 mm^2), and all of the beams have the same cross-sectional properties which will be varied in this example. The height of the frame is H = 7.315 m, and the length of each beam is also 7.315 m. Note that the purpose of this example is to demonstrate the full potential of the axial deformations to reduce the critical gravity loads when compared with ignoring them. It is presented as simply as possible in order to maintain clarity and to show that the axial beam deformations are solely responsible for the reductions to the critical loads observed. It may not be a realistic representation of frames in practice. Furthermore, although this frame does not contain diagonal bracing, the proposed method still applies via S_L = 0.

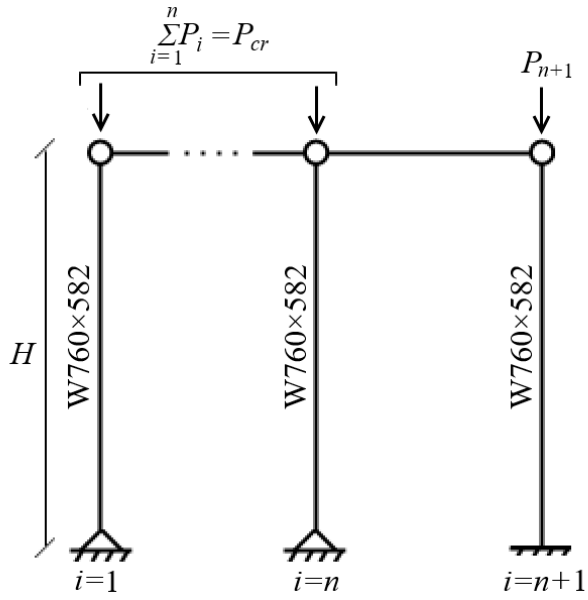

Figure 14 – Lean-on system consisting of *n* bays for Example 2

The tangent modulus model [37] in Eq. (19) is applied with E_0 = 200 GPa and f_y = 350 MPa, with the slenderness ratios of the columns being 21.5. The lean-on columns are each subjected to an axial load P_i, and the frame critical gravity load, P_{cr}, is defined as the total gravity load in the frame during which the lateral stiffness of the frame diminishes to zero. It can be shown that the lateral stiffness of a lean-on column from Eq. (3) converges to Eq. (27).

$$S_{c,i}\Big|_{r_u=r_l=0} = -P_i / H \tag{27}$$

In other words, the lateral stiffness of a lean-on column is negatively proportional to the axial load and is zero in the absence of axial loading, and is independent of the flexural stiffness (*EI*). The lean-on columns are individually stable as long as $P_i < P_u$ = 21519 kN, being braced by the cantilever, but will rotationally buckle if P_u is exceeded. The cantilever is not loaded and provides lateral support to the other columns with constant lateral stiffness $S_{c,n+1}$ = 13213 kN/m. Without considering the beam axial deformations, the lateral stiffness of the frame is given in Eq. (28).

$$\Sigma S = S_{c,n+1} - \frac{1}{H}\sum_{i=1}^{n} P_i \tag{28}$$

Since all of the columns have the same length, the critical gravity load of the frame without considering axial beam deformations is solved by setting $\Sigma S = 0$, resulting in the frame critical gravity load (summed over all columns) of $P_{cr} = HS_{c,n+1}$ = 96700 kN, which is independent of the number of bays and assumes that none of the axial loads in the lean-on columns exceed the rotational buckling load (only possible for $n \geq 5$, as rotational buckling governs the failure for $n < 5$). In this study, the number of bays was varied from n = 5 to 15, and the critical total gravity load accounting for axial beam deformations was calculated for each case. Below n = 5, it is not possible for the lateral sway buckling mode to occur due to the rotational buckling of the columns prior to the frame critical gravity load corresponding to lateral sway being reached.

The sizes of the beams were also varied using the sizes W100×19, W410×67, W610×174, W840×392 and W920×784. The cross-sectional areas of the beams are 1630 mm^2, 8600 mm^2, 22200 mm^2, 50000 mm^2 and 99800 mm^2, respectively. The reductions to the critical total load as a percentage below 96700 kN, the value without considering axial beam deformations, for each scenario are plotted in Fig. (15). Note that since in this example these beams are simply supported, their flexural stiffness (*EI*) has no effect on the connection rigidity nor lateral stiffness and storey-based stability calculations in the frame. Therefore, as intended, even though the moments of inertia of the beams vary with the section size, the changes in

the results of the critical gravity loads are purely accounted to the axial beam deformations associated with the cross-sectional areas of the beams.

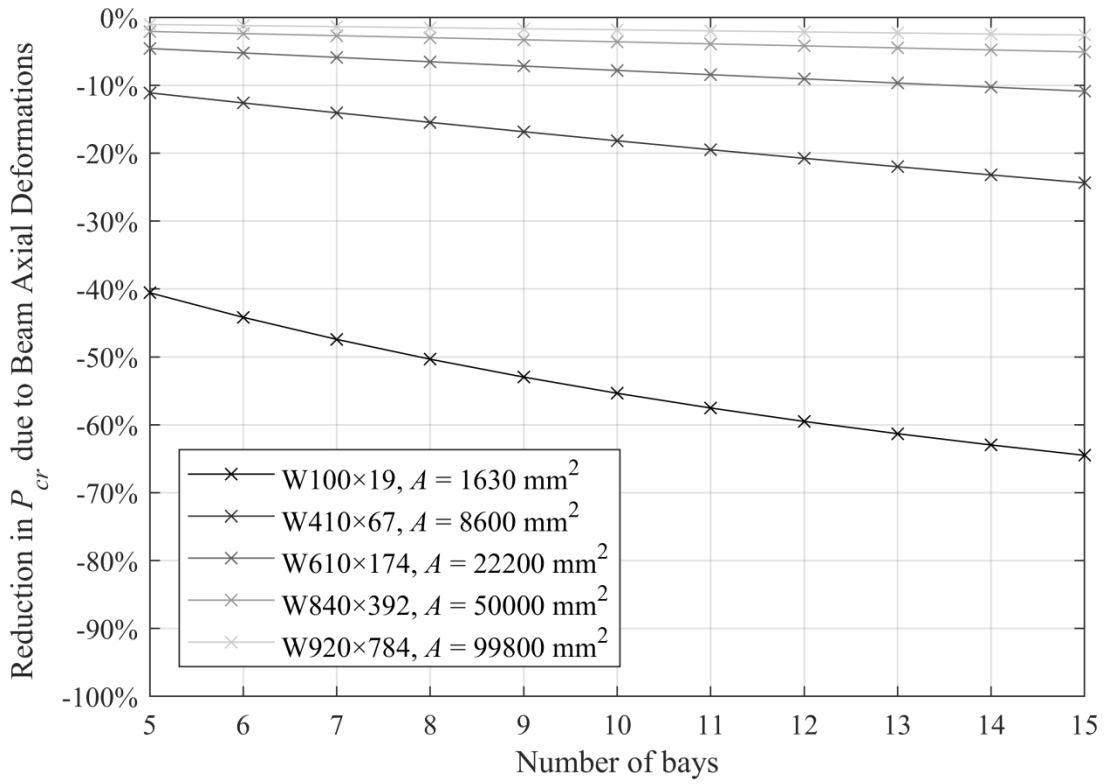

Figure 15 – Reductions to the critical total load with varying beam size and number of bays

Based on Fig. (15), the percentage reduction to the critical total load increases as more bays with lean-on columns are added to the frame. Note that a zero percent reduction corresponds to P_{cr} = 96700 kN and a 100% reduction corresponds to P_{cr} = 0. A decrease to the beam area, and consequently the beam axial lateral stiffness, also results in a reduction to P_{cr}. In each case, the ς values of the supporting column to end beam system are 3.4, 17.8, 45.9, 103.5 and 206.5 in increasing order of beam area. The ς values of the lean-on columns vary and are negative when loaded, but do not govern as the minimum ς values when considered based on absolute value. Notice that in the case of ς = 206.5 the actual reduction to P_{cr} in Fig. (15) varies from only 1.1% to 2.6%. In contrast, for the case of ς = 3.4 the reduction varies from 40.6% to 64.5%. Based on the example, the value of ς has the greatest influence on the critical total load, and the number of bays has a lesser but still significant influence.

Finally, using the same methodology presented in the previous example a finite element model was constructed using B23 elements to verify the critical gravity load for the data point corresponding to $n = 5$ and $A = 1{,}630$ mm^2 corresponding to W100×19 beams. Join + Rotation constraints were employed to model the connections. The corresponding critical gravity load obtained in FEA was 57447 kN whereas the critical gravity load obtained from the proposed method was 57445 kN (a 0.004% difference). Both of these values correspond to a 40.6% reduction to the critical gravity load as a result of considering the beam axial deformations shown in Fig. (15). The buckled shape is shown in Fig. (16), showing $n = 5$ lean-on columns and the supporting W780×582 column. As expected, the lean-on columns and beams do not bend because their ends are pin-pinned. All of the lateral resistance is provided by the bending deformation in the supporting column.

Figure 16 – Buckled shape of the lean-on frame in Example 2 with $n = 5$ bays

4.3 Example 3

Thus far, Examples 1 and 2 have demonstrated a wide range in the significance of axial deformations on the critical gravity loads of the frames (from negligible reductions in Example 1 up to a 64.5% reduction in Example 2). The purpose of Example 3 is to an example whereby the critical gravity loads of a single storey, semi-rigidly connected frame subjected to proportional loading are shown to be moderately affected by axial deformations. The first four bays of the frame are shown in Fig. (17), but the frame is symmetrical and contains a total of eleven bays (11 beams and 12 columns). All of the interior bays are identical except for the two containing diagonal bracing shown. The exterior bays are fixed at the base ($r_l = 1$), while the interior bays are pinned at the base ($r_l = 0$).

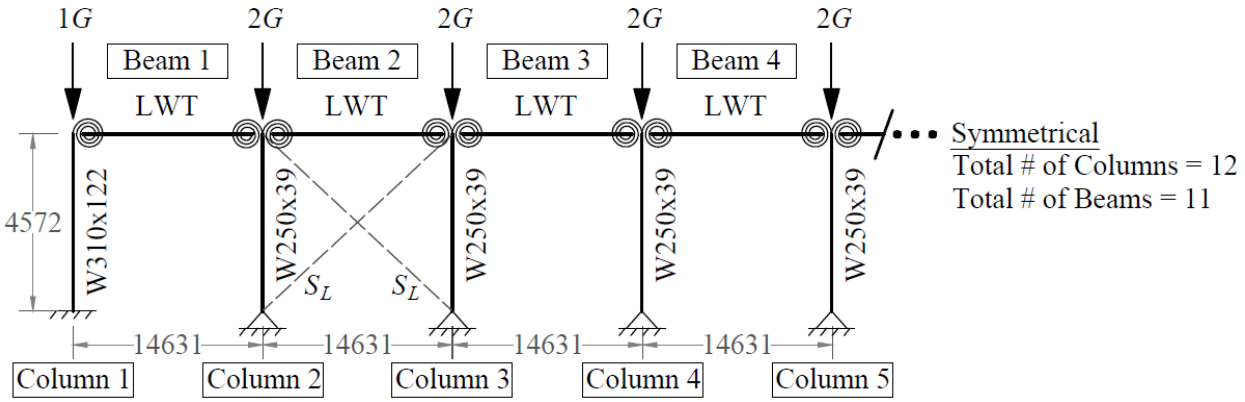

Figure 17 – Eleven-bay frame subjected to proportional gravity loading

The planar frame is located in a rectangular plan frame and the direction of analysis is such that the columns buckle about their weak axis (for W310×122, $I = 61.5\times10^6$ mm^4 and $A = 15500$ mm^2; for W250×39, $I = 5.94\times10^6$ mm^4 and $A = 4920$ mm^2). Note that the proposed method can simply be repeated for the other direction, corresponding to strong axis buckling related to the opposite plan dimension. The column slenderness ratios (L/r_g where r_g is the radius of gyration about the axis of buckling) are 73 and 132 for the exterior and interior columns, respectively. The roof rafters are lightweight steel trusses (LWT) with moment of inertia $I = 257\times10^6$ mm^4 and total top-and-bottom chord cross-sectional area $A = 4360$ mm^2. The truss-to-column connections are all semi-rigid with $r_N = r_F = 0.25$. The values of the elastic modulus for the members are calculated via the tangent modulus assumption in Eq. (19). The end connection rotation ratios are assumed to be $v_{FN} = 1$ in correspondence to the asymmetrical buckling assumption recommended in [6]. The lateral stiffness provided by the tension-only diagonal bracing, S_L, was once again varied from zero to 10,000 kN/m (which can be provided by a 33 mm diameter bar). The critical loads, G_{cr}, of the planar frame computed via the proposed method are plotted with those obtained with neglecting the effects of axial deformations via the Xu and Liu method [6] in Fig. (18).

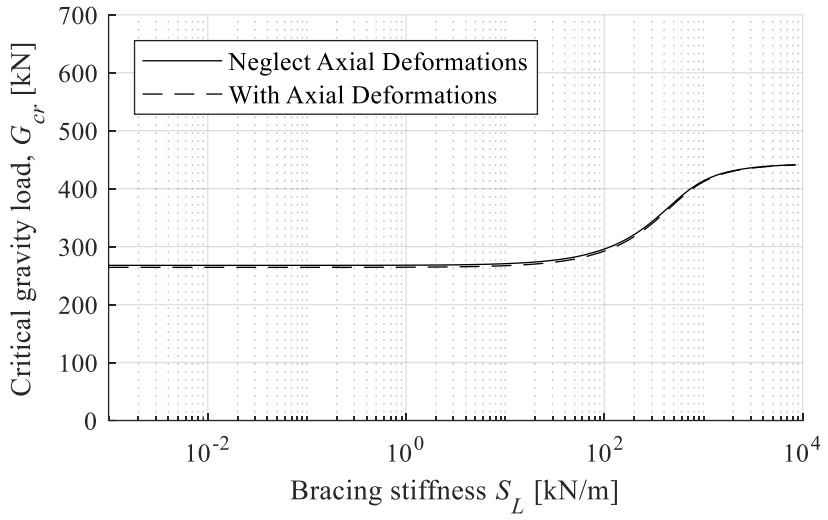

Figure 18 – Critical gravity loads of the eleven-bay frame with varying lateral bracing stiffness

Unlike the plot for Example 1 shown in Fig. (11), there is a noticeable difference in the results of the critical gravity loads when axial deformations are considered. To show the difference more clearly, Fig. (19) plots the percentage difference between the two curves from Fig. (18).

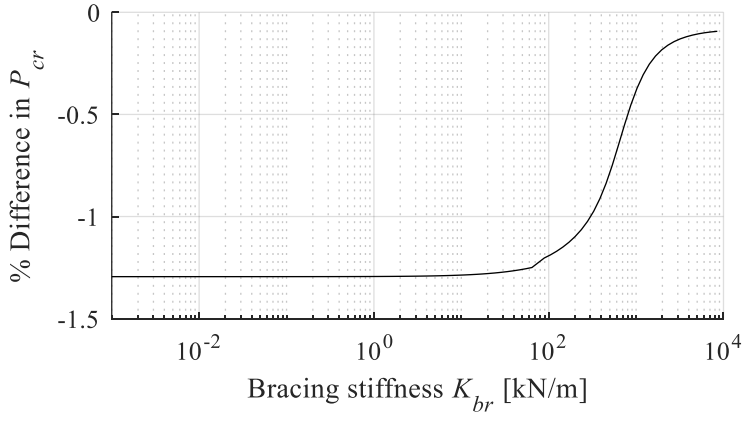

Figure 19 – Reductions of critical gravity loads for the eleven-bay frame with varying bracing stiffness

As seen in Fig. (19), the percentage reduction to the critical load due to beam axial deformations is up to 1.29% in this example, which can be considered to be significant based on the 1% threshold of significance defined in [16]. Of course, the effect of truss axial deformations on the critical gravity loads can be increased by various means, such as by adding to the number of bays in the frame or further

675 reducing the cross-sectional areas of the LWT. As with Example 1, the effect of axial beam deformations
676 becomes negligible as the frame approaches the fully-braced condition because rotational buckling is not
677 related to axial beam deformations. Note that based on Fig. (18), the frame can be considered in this case
678 to be semi-braced when S_L is between 10^2 and 10^3 kN/m. Below this range, the critical gravity load
679 approaches the unbraced case (G_{cr} = 264.2 kN considering beam axial deformations; G_{cr} = 267.7 kN
680 neglecting beam axial deformations). Above this range, the critical gravity load approaches the rotational
681 buckling case corresponding to a fully-braced frame (G_{cr} = 442 kN).
682 As with the previous examples, a finite element model of the eleven-bay frame was constructed to verify
683 the theoretical accuracy of the proposed method and derived equations. A model similar to that shown in
684 Fig. (12) but with eleven bays and semi-rigid connections via the Join+Rotation constraint was
685 established in ABAQUS [38]. This time, the rotational stiffness of the beam-to-column joints was
686 specified based on the end fixity factors. The data points on Fig. (18) corresponding to three different
687 values of S_L were verified: (a) the unbraced case, S_L = 0, (b) the semi-braced case, S_L = 220 kN/m
688 corresponding to diagonal steel tension cable braces with 3/16" diameter, and (c) the fully-braced case, S_L
689 = 10000 kN/m. In this example, the values of the end rotational stiffness of the columns $R_{u,i}$ and $R_{l,i}$ in Eq.
690 (1) are dependent on the assumed values of v_{FN} via Eq. (2). As such, the verification was completed by
691 first comparing the results of Fig. (18), obtained via assuming v_{FN} = 1, with the critical gravity loads
692 obtained in FEA. In all cases, as predicted in [6], the errors to the critical gravity loads obtained via
693 assumption of v_{FN} = 1 the proposed method were not significant. Following this comparison, the buckled
694 shapes of the frames obtained via the FEA solutions of critical gravity loads were obtained, and the joint
695 rotations at the upper ends of each column were recorded. Based on these joint rotations, calibrated values
696 of v_{FN} corresponding to the buckled shape and critical gravity loads were obtained by dividing the far end
697 rotations by the near end rotations for each beam. The calibrated values of v_{FN} were then re-substituted
698 back to the proposed equations, with which the critical gravity loads were re-calculated and compared
699 with the FEA solution. The results of this analysis are summarized in Table 2.

Table 2. Validation of critical gravity loads, G_{cr} (kN), obtained from proposed method using FEA for Example 3

Diag. Bracing Stiffness	No Axial Deformations Considered			Axial Deformations Considered		
	FEA	Xu & Liu [6] (v_{FN} = 1)	Xu & Liu [6] (v_{FN} calib.)	FEA	Proposed Method (v_{FN} = 1)	Proposed Method (v_{FN} calib.)
S_L = 0.0 kN/m	260.764	267.642	260.745	257.545	264.179	257.528
S_L = 220 kN/m	319.192	325.178	319.175	315.858	321.668	315.842
S_L = 10,000 kN/m	439.768	441.358	439.760	439.568	440.959	439.639
Column Reference	1	2	3	4	5	6

When comparing the un-calibrated results (v_{FN} = 1) with the corresponding FEA results in Table 2 (between columns 1 and 2, and between columns 4 and 5), the maximum error is within 3%, which is expected given that the assumption of v_{FN} = 1 does not correspond to the actual buckled shape of the frame. When comparing the calibrated results in Table 2 with the corresponding FEA results (between columns 1 and 3, and between columns 4 and 6), the error is within 0.02%, indicating that the proposed equations are accurate to the theoretical solutions. In terms of the effect of beam axial deformations on the critical gravity loads of the frame, the corresponding reductions to the critical gravity loads obtained in FEA (comparing columns 1 and 4) are 1.23%, 1.04%, and 0.03% for the unbraced, semi-braced and fully-braced cases, respectively. These values are considerably accurate to those shown in Fig. (19). For the unbraced case, during the failure at 257.5 kN considering axial deformations, the minimum value of ς in the frame is 108. Similarly, during the failure at 315.8 kN for the semi-braced case, the minimum value of ς in the frame is 111. Based on Fig. (9), these values can be correctly used to predict that the effect of axial deformations has approximately 1% influence on the critical gravity loads in the unbraced and semi-braced cases. However, for the fully-braced case, axial deformations do not significantly affect the critical gravity loads because rotational buckling is imminent, regardless of the values of ς. Finally, the buckled shapes obtained from the finite element analyses for the unbraced, semi-braced, and fully-braced cases are shown in Figs. (20a), (20b) and (20c), respectively.

Figure 20(a) – Buckled shape of the eleven-bay frame with S_L = 0.0 kN/m (unbraced)

Figure 20(b) – Buckled shape of the eleven-bay frame with S_L = 220 kN/m (semi-braced)

Figure 20(c) – Buckled shape of the eleven-bay frame with S_L = 10000 kN/m (fully-braced)

The buckling shapes shown in Figs. (20) are extracted directly from the output of ABAQUS [38]. The bracing bays are located on the second and tenth bays, but are not shown as the braces have been modelled as equivalent springs. Similar to Example 1, the lateral sway mode is experienced by the frame in the unbraced and semi-braced cases, whereas the rotational buckling of the individual columns governs in the fully-braced case. Note that the relative magnitudes of column curvature corresponding to the semi-braced case are greater than those observed in the unbraced case. Finally, it is noted that if the values of the end fixity factors were increased to 0.75, the effect of axial beam deformations would account for up to a 1.64% difference to the critical load, experienced during the unbraced case (S_L = 0) and obtained using the assumption of v_{FN} = 1 under the proposed method. The critical loads obtained with and without considering the axial deformations would be 352.5 kN and 358.4 kN, respectively.

5 Conclusion

A method has been proposed in this paper for evaluating the storey-based stability of semi-braced and unbraced steel frames containing idealized or semi-rigid connections, using the concept of equivalent spring stiffness. The method is also theoretically validated via finite element analysis. Based on the examples presented, the conclusions of this study are summarized as follows:

- The effect of beam axial deformations always reduces the lateral stiffness, and consequently, the critical gravity loads of a frame. As such, should not always be neglected during structural analysis.

- The relative influence of beam axial deformations on the critical gravity loads in unbraced and semi-braced frames can be predicted using the proposed local stiffness reduction factor, ς. A value of ς within the order of 10^2 or less indicates that beam axial deformations can significantly affect the critical gravity loads unless rotational buckling (indicative of a fully-braced frame) governs the failure mode. This fact can be used as a simple check for designers to verify whether axial deformations should be considered in an analysis.
- Increasing the number and/or lengths of beams in a frame was also found to increase the influence of axial beam deformations on the lateral stiffness of the frame.
- The lateral stiffness and stability of a semi-braced or unbraced frame can be assessed using the equivalent spring stiffness method. As the equivalent spring stiffness method is easy to understand it can be useful for teaching and understanding the behaviour of structural systems, and used in future design methodologies.
- The proposed method is shown to be theoretically accurate via a series of finite element analyses conducted on the numerical examples. As such, it may prove advantageous over the use of sophisticated numerical analysis packages which have their own theoretical assumptions and limitations.

Some limitations of this study include the fact that it relies on various assumptions such as tension-only bracing, use of empirical inelasticity models, and inter-storey interactions in multistorey buildings. Nevertheless, it represents a necessary step towards providing comprehensive and practical global stability analysis tools for steel structures. In terms of future work, it is recommended to experimentally validate the theoretical results presented in this study.

Appendix A Derivation of Lateral Stiffness for a Column

This appendix overviews the theoretical basis for Eq. (3), which was derived by Xu & Liu [6]. For the semi-rigidly connected and axially loaded column in Figure 21, a lateral deflection Δ is assumed to occur.

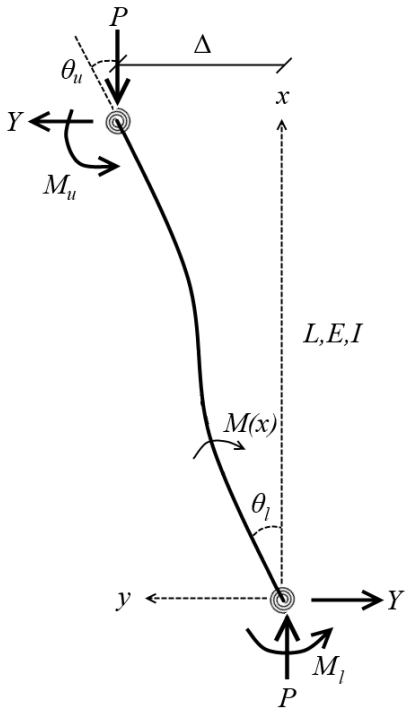

768

769 **Figure 21 – *P*-Δ analysis of a semi-rigidly connected column**

770 The resulting lateral reactions Y and end moments M_u and M_l can be expressed in the force balance
771 equation Eq. (29). Note that the end moments are shown in the positive counter-clockwise convention but
772 act in the opposite direction.

773 $$M_u + M_l = YL + P(\Delta + \Delta_0) \tag{29}$$

774 The end moments M_u and M_l relate to the additional end rotations, θ_l and θ_u, in Eq. (30).

775 $$M_u = R_u\theta_u; \quad M_l = R_l\theta_l \tag{30}$$

776 The governing differential equation is given in Eq. (31).

777 $$EI\frac{d^2y}{dx^2} = \theta_l R_l - Py - Yx \tag{31}$$

778 Solving the differential equation results in the deformed shape functions and bending moment function in
779 Eqs. (32).

780 $$y(x) = C_1\cos\left(\frac{\phi}{L}x\right) + C_2\sin\left(\frac{\phi}{L}x\right) + \frac{M_l}{P} - \frac{Y}{P}x \tag{32a}$$

781 $$y'(x) = C_2\frac{\phi}{L}\cos\left(\frac{\phi}{L}x\right) - C_1\frac{\phi}{L}\sin\left(\frac{\phi}{L}x\right) - \frac{Y}{P} \tag{32b}$$

$$M(x) = -P\left(C_1 \cos\left(\frac{\phi}{L}x\right) + C_2 \sin\left(\frac{\phi}{L}x\right)\right) \tag{32c}$$

where C_1 and C_2 are integration constants. There are four boundary conditions to this problem, listed in Eqs. (33).

$$y(0) = 0 \tag{33a}$$
$$y(L) = \Delta \tag{33b}$$
$$y'(0) = \theta_l \tag{33c}$$
$$y'(L) = \theta_u \tag{33d}$$

The solution to the system of five equations comprising of Eq. (29) and Eqs. (33) is expressed in Eq. (34), which is represented as $S_{c,i}$ in Eq. (3).

$$\frac{Y}{\Delta} = \frac{12EI}{L^3}\beta \tag{34}$$

Acknowledgements

The authors wish to thank the National Science and Engineering Research Council of Canada (NSERC) (RGPIN-203154-2013) for the financial support of this work.

References

1. Yura JA. The effective length of columns in unbraced frames. Engrg J 1971; 8(2):37-42.
2. LeMessurier W. A practical method of second order analysis Part 2 - Rigid Frames. Engrg J 1977; 14(2):49-67.
3. Lui EM. A novel approach for K factor determination. Engrg J 1992; 29:150-159.
4. Aristizabal-Ochoa, JD. Storey stability of braced, partially braced, and unbraced frames: classical approach. J Struct Engrg 1997; 123(6):799-807.
5. Xu L. The buckling loads of unbraced PR frames under non-proportional loading. J Constr Steel Res 2001; 58:443-465.
6. Xu L, Liu Y. Storey-based effective length factors for unbraced PR frames. Engrg J 2002; 39(1):13-29.

7. Blostotsky B, Efraim E, Ribakov Y. Improving the reliability of measuring critical buckling in sway mode frames. Experimental Mechanics 2016; 56: 311-321.
8. Krystosik P, On stability of unbraced steel frames with semi-rigid joints, Eurosteel 2017; Copenhagen, Denmark.
9. Gunaydin A, Aydin R. A simplified method for instability and second-order load effects of framed structures: Story-based approach. Struct Design Tall and Sp Bldgs 2019; 28(4): 1-23.
10. Hellesland J. New and extended design moment formulations for slender columns in frames with sway. Engrg Struct 2020; 109804.
11. Liu Y, Xu L. Storey-based stability of multi-storey unbraced frames. Struct Engrg Mech 2005; 19(6): 679-705.
12. Georgios EM, Gantes CJ. Buckling strength of multi-story sway, non-sway and partially-sway frames with semi-rigid connections. J Constr Steel Res 2006; 62(2006): 893-905.
13. Hellesland J. Extended second order approximate analysis of frames with sway-braced column interaction. J Constr Steel Res 2009; 65(2009): 1075-1086.
14. Li Q, Zou A, Zhang H. A simplified method for stability analysis of multi-story frames considering vertical interactions between stories. Adv Struct Engrg 2016; 19(4): 599-610.
15. Ma, T, Xu, L. Storey-based stability of unbraced steel frames under piece-linear temperature distributions. Engrg Struct 2019; 194(2019): 147-160.
16. Ma T, Xu L. Shear deformation effects on stability of unbraced steel frames in variable loading. J Constr Steel Res 2019; 164(2020): 105811.
17. Tedesco JW, McDougal WG, Ross CA. *Structural Dynamics: Theory and Applications*. 1999, Menlo Park: Addison-Wesley.
18. Weggel DC, Boyajian DM, Chen SE. Modelling of structures as systems of springs. World Transactions on Engineering and Technology Education 2007; 6(1):169-172.
19. Ziemian R. Guide to Stability Design Criteria for Metal Structures 2010; Wiley & Sons Ltd, 6th edition.

20. Ma T, Xu L. The stability of semi-braced steel frames containing members with stepped segments. Proceedings of the SDSS 2019 International Colloquium on Ductility of Steel Structures 2019; 727-734, Prague, Czechia.
21. Monforton G, Wu T. Matrix analysis of semi-rigidly connected frames. J Struct Div 1963; 89(6):13-42.
22. Bahaz A, Amara S, Jaspart JP, Demonceau JF. Analysis of the behaviour of semi rigid steel end plate connections. MATEC Web of Conferences 2017; 02058(2018): 1-6.
23. Ivanyi M. Full-scale tests of steel frames with semi-rigid connections. Engrg Struct 2000; 22(2): 168-179.
24. Al-Jabri K, Burgess I, Lennon T, Plank R. Moment-rotation-temperature curves for semi-rigid joints. J Constr Steel Res 2005; 61(2005): 281-303.
25. Bayo E, Cabrero JM, Gil B. An effective component-based method to model semi-rigid connections for the global analysis of steel and composite structures. Engrg Struct 2006; 28(1): 97-108.
26. Valipour HR, Bradford M. An efficient compound-element for potential progressive collapse analysis of steel frames with semi-rigid connections. Finite Elem Anal Des 2012; 60: 35-48.
27. Meghezzi-Larafi I, Tati A. The effective length estimation of columns in semi-rigid jointed braced frames. J Appl Engrg Sci Tech 2016; 2(2): 91-97.
28. Meirovitch L. *Dynamics and Control of Structures*. 1990, Jon Wiley & Sons.
29. Bratland M, Haugen B, Rølvåg T. Modal analysis of active flexible multibody systems. Computers & Structures 2011; 89(9-10): 750-761.
30. Alkhatib R, Golnaraghi MF. Active structural vibration control: A review. The Shock and Vibration Digest 2003; 35(5): 367-383.
31. De la Cruz ST, Rodríguez MA, Hernández V. Using spring-mass models to determine the dynamic response of two-story buildings subjected to lateral loads. 15th World Conference on Earthquake Engineering 2012: Lisbon, Portugal.

32. Hellesland J, Bjorhovde R Improved frame stability analysis with effective lengths. J Struct Engrg 1996; 122(11): 1275-1283.
33. Ma, T. *The Storey-Based Stability of Steel Frames Subjected to Variable Gravity and Fire Loading* (PhD Thesis). 2020, University of Waterloo, Canada.
34. Ypma TJ. Historical development of the Newton-Raphson method. SIAM Review 1995; 37(4):531-551.
35. Xu L. A NLP approach for evaluating storey-buckling strengths of steel frames under variable loading. Struct Multidiscip O 2003; 25(2):141-150.
36. Newmark N. A simple approximate formula for effective end-fixity of columns. J Aeronaut Sci 1949; 16(2):116.
37. Yura JA, Helwig TA. Bracing for stability. American Institute of Steel Construction; 1995.
38. Simulia. *ABAQUS Verification Guide (version 6.14)*, 2014. Providence, RI.